

Estimation of Semileptonic Decays of B_c Meson to S-wave Charmonia with NRQCD

Cong-Feng Qiao^{1,2*} and Rui-Lin Zhu^{1†}

¹*Department of Physics,
Graduate University of the Chinese Academy of Sciences,
YuQuan Road 19A, Beijing 100049, China*
²*Kavli Institute for Theoretical Physics China,
the Chinese Academy of Sciences, Beijing 100190, China*

We study the semileptonic differential decay rates of B_c meson to S-wave charmonia, η_c and J/Ψ , at the next-to-leading order accuracy in the framework of NRQCD. In the heavy quark limit, $m_b \rightarrow \infty$, we obtain analytically the asymptotic expression for the ratio of NLO form factor to LO form factor. Numerical results show that the convergence of the ratio is perfect. At the maximum recoil region, we analyze the differential decay rates in detail with various input parameters and polarization for J/ψ , which can now be checked in the LHCb experiment.

PACS numbers 12.38.Bx, 12.39.St 13.20.-v

I. INTRODUCTION

Hadron collider provides a large amount of data on B_c events. Wherein the most easily identified decay modes to tag the B_c are: fully reconstructed channel $B_c \rightarrow J/\Psi\pi$ and semileptonic decay channel $B_c \rightarrow J/\Psi\ell\nu$ ($\ell = e, \mu$). The CDF Collaboration made the first observation of the B_c meson by the semileptonic decay channel at the Tevatron fourteen years ago [1]. Latter, the D0 Collaboration performed the same analysis in a sample of 210 pb⁻¹ of the Run II data [2]. The cross section of B_c production at the Large Hadron Collider(LHC) is larger than that at the Tevatron by roughly an order of magnitude, which reaches 49.8 nb at the center-of-mass energy $\sqrt{s} = 14$ TeV [3, 4]. This makes the experimental study of the differential branching fraction of B_c meson semileptonic decays to charmonium feasible. We can also obtain the information of the Cabibbo-Kobayashi-Mashkawa(CKM) matrix element in B_c decays, especially V_{cb} which is not well determined.

Recently, the BABAR collaboration measured the partial branching fraction $\Delta B/\Delta q^2$ in bins of the momentum-transfer squared, with 6 q^2 bins for $B^0 \rightarrow \pi^-\ell^+\nu$ and 3 q^2 bins for $B^0 \rightarrow \rho^-\ell^+\nu$ [5]. They found that the partial branching fraction of $B^0 \rightarrow \pi^-\ell^+\nu$ decreases as q^2 increases, while for $B^0 \rightarrow \rho^-\ell^+\nu$ process, the partial branching fraction increases first and then decreases as q^2 increases. Actually, we know that all of the five form factors in above two decay channels at the maximum recoil region increases with q^2 , at the next-to-leading order(NLO) accuracy according to the light cone sum rules calculation [6, 7]. The decrease of $B^0 \rightarrow \pi^-\ell^+\nu$ is caused by the phase space, which counteracts the enhancement from form factors. In this work, we try to make out whether this happens or not in B_c semileptonic decays to charmonia.

There exist several approaches in calculating the B_c meson semileptonic decays to charmonium. Some of them are: the light cone QCD sum rules [8–11], the relativistic quark model [12, 13], the instantaneous non-relativistic approach to the Bethe-Salpeter equation [14], the non-relativistic constituent quark model[16], the covariant light front model [15], and the QCD potential model [17].

Consider that the B_c meson is constituted by two heavy quarks with different flavors, which masses are much larger than the Λ_{QCD} , analogous to the situation of heavy quarkonium, the system turns out to be non-relativistic. Hence the relative velocity of heavy quarks within the B_c meson is small, i.e. $v \ll 1$, though bigger than the velocities of quarks in charmonium and bottomonium systems, and the non-relativistic QCD(NRQCD) formalism is applicable to the study of B_c meson semileptonic decays to charmonia. In the NRQCD framework, the matrix elements of the concerned processes can be factorized as

$$\langle J/\psi(\eta_c)\ell\nu|\bar{c}\Gamma_\mu b\bar{\ell}\Gamma^\mu\nu|B_c\rangle \simeq \sum_{n=0} \psi(0)_{B_c}\psi(0)_{J/\psi(\eta_c)}T^n. (1)$$

Here, $\Gamma^\mu = \gamma^\mu(1 - \gamma_5)$, the nonperturbative parameters $\psi(0)_{B_c}$ and $\psi(0)_{J/\psi(\eta_c)}$ are the Schrödinger wave functions at the origin for $b\bar{c}$ and $c\bar{c}$ systems, respectively. T^n are hard scattering kernels which can be calculated perturbatively.

The paper is organized as follows: In section II we present the definition for relevant form factors and work out the expressions of form factors in the NRQCD framework. The dependence of the NLO semileptonic differential decay rates on q^2 is also obtained. In section III we study the theoretical uncertainty, and analyze the result in detail of the maximum recoil region. The last section is remained for conclusions.

*email:qiaocf@gucas.ac.cn

†email:zhuruilin09@mails.gucas.ac.cn

II. FORM FACTORS AND SEMILEPTONIC DIFFERENTIAL DECAY RATES IN THE NRQCD FRAMEWORK

The $B_c \rightarrow J/\psi(\eta_c)$ transition form factors, f_+ , f_0 , V , A_0 , A_1 , and A_2 are normally defined as follows [18]

$$\begin{aligned} \langle \eta_c(p) | \bar{c} \gamma^\mu b | B_c(P) \rangle &= f_+(q^2) (P^\mu + p^\mu - \frac{m_{B_c}^2 - m_{\eta_c}^2}{q^2} q^\mu) \\ &+ f_0(q^2) \frac{m_{B_c}^2 - m_{\eta_c}^2}{q^2} q^\mu, \end{aligned} \quad (2)$$

$$\begin{aligned} \langle J/\psi(p, \varepsilon^*) | \bar{c} \gamma^\mu b | B_c(P) \rangle &= \frac{2iV(q^2)}{m_{B_c} + m_{J/\psi}} \epsilon^{\mu\nu\rho\sigma} \varepsilon_\nu^* p_\rho P_\sigma, \\ \langle J/\psi(p, \varepsilon^*) | \bar{c} \gamma^\mu \gamma_5 b | B_c(P) \rangle &= 2m_{J/\psi} A_0(q^2) \frac{\varepsilon^* \cdot q}{q^2} q^\mu \\ &- A_2(q^2) \frac{\varepsilon^* \cdot q}{m_{B_c} + m_{J/\psi}} (P^\mu + p^\mu - \frac{m_{B_c}^2 - m_{J/\psi}^2}{q^2} q^\mu) \end{aligned}$$

$$+ (m_{B_c} + m_{J/\psi}) A_1(q^2) (\varepsilon^{*\mu} - \frac{\varepsilon^* \cdot q}{q^2} q^\mu). \quad (3)$$

Here we define the momentum transfer $q = P - p$. Note that $f_0(0) = f_+(0)$ at the maximum recoil.

It is straightforward to calculate those form factors at the tree level in the NRQCD. They read

$$V^{LO}(q^2) = \frac{16\sqrt{2}C_A C_F \pi (3z+1) \alpha_s \psi(0)_{B_c} \psi(0)_{J/\Psi}}{(q^2 - (z-1)^2)^2 \left(\frac{z}{z+1}\right)^{3/2} m_b^3 N_c}, \quad (4)$$

$$A_0^{LO}(q^2) = \frac{16\sqrt{2}C_A C_F \pi (z+1)^{5/2} \alpha_s \psi(0)_{B_c} \psi(0)_{J/\Psi}}{(q^2 - (z-1)^2)^2 z^{3/2} m_b^3 N_c}, \quad (5)$$

$$A_1^{LO}(q^2) = \frac{16\sqrt{2}C_A C_F \pi \sqrt{z+1} (4z^3 + 5z^2 + 6z - q^2(2z+1) + 1) \alpha_s \psi(0)_{B_c} \psi(0)_{J/\Psi}}{(q^2 - (z-1)^2)^2 z^{3/2} (3z+1) m_b^3 N_c}, \quad (6)$$

$$A_2^{LO}(q^2) = \frac{16\sqrt{2}C_A C_F \pi \sqrt{z+1} (3z+1) \psi(0)_{B_c} \psi(0)_{J/\Psi}}{(q^2 - (z-1)^2)^2 z^{3/2} m_b^3 N_c}, \quad (7)$$

$$f_+^{LO}(q^2) = \frac{8\sqrt{2}C_A C_F \pi \sqrt{z+1} (-q^2 + 3z^2 + 2z + 3) \alpha_s \psi(0)_{B_c} \psi(0)_{\eta_c}}{(q^2 - (z-1)^2)^2 z^{3/2} m_b^3 N_c}, \quad (8)$$

$$f_0^{LO}(q^2) = \frac{8\sqrt{2}C_A C_F \pi \sqrt{z+1} (9z^3 + 9z^2 + 11z - q^2(5z+3) + 3) \alpha_s \psi(0)_{B_c} \psi(0)_{\eta_c}}{(q^2 - (z-1)^2)^2 z^{3/2} (3z+1) m_b^3 N_c}, \quad (9)$$

where $z \equiv m_c/m_b$.

In Ref. [19, 20], the form factors of B_c transition to η_c with alternative parameterizations had been calculated at the NLO accuracy in the non-relativistic limit. There are three typical scales of the process, which possess the hierarchy of $\Lambda_{QCD} \ll m_c \ll m_b$. Taking into account the work of Ref. [21], where the NLO form factors of B_c transition to J/Ψ are calculated, we expand the ratios of the NLO form factors to the leading order(LO) form factors at first order in $z = m_c/m_b$ expansion in the heavy quark limit $m_b \rightarrow \infty$. And the asymptotic expressions of which are then obtained analytically, that can be found in the Appendix A.

For light leptons ($\ell = e, \mu$), their masses m_ℓ can be readily neglected, hence the semileptonic differential de-

cay rate of $B_c \rightarrow \eta_c \ell \nu$ depending on q^2 reads

$$\frac{d\Gamma}{dq^2}(B_c \rightarrow \eta_c \ell \nu) = \frac{G_F^2 |V_{cb}|^2}{192\pi^3 m_{B_c}^3} \lambda(q^2)^{3/2} [f_+(q^2)]^2. \quad (10)$$

Here, G_F is the Fermi constant; V_{cb} is the CKM matrix element; and $\lambda(q^2) = (m_{B_c}^2 + m_{\eta_c}^2 - q^2)^2 - 4m_{B_c}^2 m_{\eta_c}^2$. For lepton τ , its mass can not be ignored in the analysis, in which the form factors f_0 and f_+ are both involved in. Thus f_0 can be measured via $B_c \rightarrow \eta_c \tau \nu_\tau$ process while f_+ is obtained in $B_c \rightarrow \eta_c \ell \nu_\ell$ decay.

By virtue of the NLO form factors, we can easily gain the distribution of NLO differential decay rate on momentum transfer q^2 . To check the convergence behavior of the ratio of NLO differential decay rate to LO one, we select three sets of different values of z and scale q^2 , and illustrate parameter dependence in the first diagram

TABLE I: Theoretical parameters for different sets, with renormalization scale $\mu = 4.8$ GeV, the lifetime of the B_c $\tau(B_c) = 0.453$ ps, and $G_F = 1.16637 \times 10^{-5}$ GeV $^{-2}$ [22], where m_b , m_c and Λ are given in GeV, while $|\psi(0)|$ are given in GeV $^{3/2}$ [23, 24].

	m_b	m_c	Λ	$ \psi(0) _{B_c}$	$ \psi(0) _{\eta_c}$	$ \psi(0) _{J/\Psi}$
set 1	4.8	1.5				
set 2	4.9	1.4	0.10	0.3615	0.283	0.283
set 3	5.0	1.3				

of Fig 1. The parameters in the three typical choices can be found in Table I, wherein the Schrödinger wave functions at the origin for J/Ψ are determined through their leptonic decay widths at NLO.

For $B_c \rightarrow \eta_c \ell \nu$ channel, at the maximum recoil point $q^2 = 0$, we obtain a value $4.67^{+0.38}_{-0.58} \times 10^{-12} |V_{cb}|^2$ GeV $^{-1}$ for (10), which is larger than the value of $0.65 \times 10^{-12} |V_{cb}|^2$ GeV $^{-1}$ obtained in nonrelativistic quark model [16]. Besides, the results away from the maximum recoil point tend to disagree with what in Ref. [16]. In NRQCD calculation, the form factors of B_c to η_c are obviously enhancing with q^2 increase, than other approaches light cone sum rules and nonrelativistic quark model, and the trend is sharpening at NLO, which counteracts the decrease from the factor of phase space.

For the channel of $B_c \rightarrow J/\Psi \ell \nu$ ($\ell = e, \mu$), the decay rates in transverse and longitudinal polarization of vector meson J/Ψ can be formulated as

$$\frac{d\Gamma_L}{dq^2} = \frac{G_F^2 \lambda(q^2)^{1/2} |V_{cb}|^2 q^2}{192\pi^3 m_{B_c}^3} |H_0(q^2)|^2, \quad (11)$$

$$\frac{d\Gamma_T}{dq^2} = \frac{G_F^2 \lambda(q^2)^{1/2} |V_{cb}|^2 q^2}{192\pi^3 m_{B_c}^3} (|H_+(q^2)|^2 + |H_-(q^2)|^2), \quad (12)$$

respectively. Here the helicity amplitudes are expressed as follows:

$$H_{\pm}(q^2) = \frac{\lambda(q^2)^{1/2}}{m_{B_c} + m_{J/\Psi}} \left[V(q^2) \mp \frac{(m_{B_c} + m_{J/\Psi})^2}{\lambda(q^2)^{1/2}} A_1(q^2) \right], \quad (13)$$

$$H_0(q^2) = \frac{1}{2m_{J/\Psi} \sqrt{q^2}} \left[-\frac{\lambda(q^2)}{m_{B_c} + m_{J/\Psi}} A_2(q^2) + (m_{B_c} + m_{J/\Psi})(m_{B_c}^2 - m_{J/\Psi}^2 - q^2) A_1(q^2) \right]. \quad (14)$$

While summing up the various polarizations, the semileptonic differential decay rate of $B_c \rightarrow J/\Psi \ell \nu$ over q^2 is obtained

$$\frac{d\Gamma}{dq^2}(B_c \rightarrow J/\Psi \ell \nu) = \frac{G_F^2 \lambda(q^2)^{1/2} |V_{cb}|^2 q^2}{192\pi^3 m_{B_c}^3} \times (|H_+(q^2)|^2 + |H_-(q^2)|^2 + |H_0(q^2)|^2), \quad (15)$$

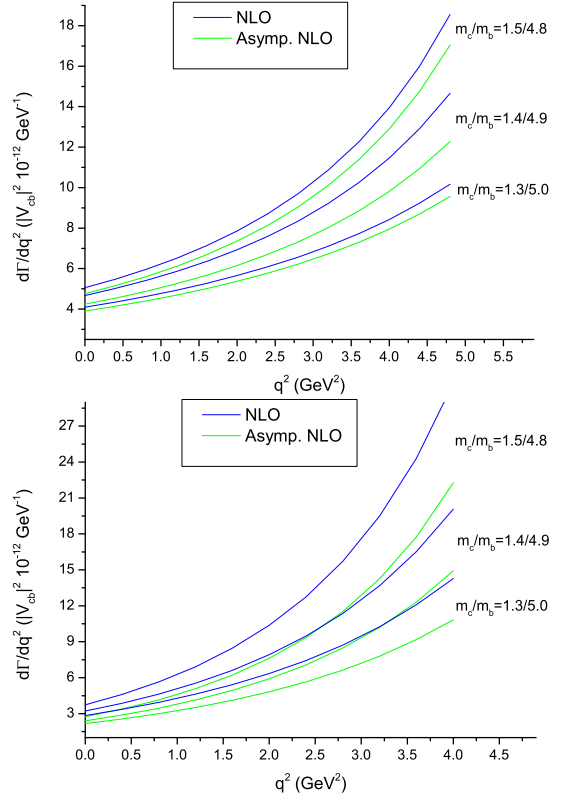


FIG. 1: NLO differential decay rates for the $B_c \rightarrow \eta_c \ell \nu$ (up) and $B_c \rightarrow J/\Psi \ell \nu$ (down), for different values of quark mass. The renormalization scale is chosen to be close to the bottom quark mass, i.e. $\mu = 4.8$ GeV. In the figure, Asympt. NLO means expanding the ratio of NLO form factor to LO one at the first order in $z = m_c/m_b$ expansion and in the heavy quark limit $m_b \rightarrow \infty$.

where $\lambda(q^2) = (m_{B_c}^2 + m_{J/\Psi}^2 - q^2)^2 - 4m_{B_c}^2 m_{J/\Psi}^2$.

Similar as $B_c \rightarrow \eta_c \ell \nu$, the distribution of NLO differential decay rate on momentum transfer q^2 for $B_c \rightarrow J/\Psi \ell \nu$ channel with three sets of different values of z is illustrated in the low diagram of Fig. 1. At the maximum recoil point $q^2 = 0$, we obtain a value of $3.21^{+0.53}_{-0.37} \times 10^{-12} |V_{cb}|^2$ GeV $^{-1}$ for (15), which is larger than the value of $0.6 \times 10^{-12} |V_{cb}|^2$ GeV $^{-1}$ obtained in nonrelativistic quark model [16]. Except for the enhancement from the NLO K-factor and the NLO Schrödinger wave functions at the origin, the result in LO in NRQCD calculation is intrinsically bigger than what obtained in nonrelativistic quark model.

III. THEORETICAL UNCERTAINTY

In this section, the theoretical uncertainties of the NLO semileptonic decay rates in maximum recoil region are investigated in detail. It is found that the main uncertainties of the concerned processes have two sources, the heavy quark masses and the renormalization scale. In the

TABLE II: The NLO partial decay width for various q^2 . Herein, ℓ may be any kind of light leptons, the e or μ . We take $m_c/m_b = 1.4/4.9$, $\mu = 4.8$ GeV in the evaluation. The uncertainty in the first column of the value comes from varying the ratio of quark masses m_c/m_b from 1.5/4.8 to 1.3/5.0; while the uncertainty in the second column comes from varying the renormalization scale μ from 3 GeV to 6 GeV. For J/Ψ , the partial decay widths in transverse(ε_\perp^*) and longitudinal polarization(ε_\parallel^*) of J/Ψ are presented separately.

bins of q^2 (GeV ²)	$0 \leq q^2 \leq 1$	$1 \leq q^2 \leq 2$	$2 \leq q^2 \leq 3$	$3 \leq q^2 \leq 4$	$4 \leq q^2 \leq 5$
$\Delta\Gamma(B_c \rightarrow \eta_c \ell \nu) (10^{-15} \text{ GeV})$	$8.06^{+1.17+1.96}_{-0.77-0.74}$	$9.73^{+1.78+2.37}_{-1.16-0.89}$	$12.0^{+2.78+2.95}_{-1.77-1.11}$	$15.2^{+4.47+2.73}_{-3.77-1.41}$	$20.0^{+7.57+5.06}_{-4.36-1.87}$
$\Delta\Gamma(B_c \rightarrow J/\Psi(\varepsilon_\perp^*)\ell\nu) (10^{-15} \text{ GeV})$	$0.70^{+0.215+0.159}_{-0.141-0.061}$	$2.64^{+0.95+0.60}_{-0.60-0.23}$	$5.84^{+2.54+1.34}_{-1.51-0.51}$	$11.28^{+6.03+2.61}_{-3.35-1.00}$	$20.97^{+14.14+4.90}_{-7.16-1.87}$
$\Delta\Gamma(B_c \rightarrow J/\Psi(\varepsilon_\parallel^*)\ell\nu) (10^{-15} \text{ GeV})$	$6.01^{+1.14+1.40}_{-0.78-0.53}$	$7.87^{+1.93+1.84}_{-1.27-0.70}$	$10.64^{+3.38+2.51}_{-2.72-0.95}$	$14.96^{+6.18+3.56}_{-3.62-1.35}$	$22.07^{+12.06+5.31}_{-6.45-2.01}$
$\Delta\Gamma(B_c \rightarrow J/\Psi \ell \nu) (10^{-15} \text{ GeV})$	$6.71^{+1.35+1.56}_{-0.92-0.59}$	$10.52^{+2.89+2.45}_{-1.88-0.93}$	$16.49^{+5.92+3.86}_{-4.24-1.47}$	$26.24^{+12.21+6.18}_{-6.98-2.35}$	$43.04^{+26.20+10.22}_{-13.61-3.88}$

TABLE III: The NLO partial decay width of processes $B_c \rightarrow \eta_c \tau \nu_\tau$ and $B_c \rightarrow J/\Psi \tau \nu_\tau$ for various q^2 , where the maximum recoil point is at m_τ^2 . We take the value of $m_\tau^2 = 1.776^2$ GeV².

bins of q^2 (GeV ²)	$m_\tau^2 \leq q^2 \leq 4$	$4 \leq q^2 \leq 5$
$\Delta\Gamma(B_c \rightarrow \eta_c \tau \nu_\tau) (10^{-15} \text{ GeV})$	$2.460^{+0.9245+0.655}_{-0.538-0.241}$	$17.62^{+8.42+4.70}_{-4.56-1.73}$
$\Delta\Gamma(B_c \rightarrow J/\Psi \tau \nu_\tau) (10^{-15} \text{ GeV})$	$0.821^{+0.375+0.194}_{-0.213-0.073}$	$6.922^{+4.017+1.648}_{-2.107-0.625}$

evaluation, we vary the charm quark mass $m_c = 1.4$ GeV by ± 0.1 GeV, the bottom quark mass $m_b = 4.9$ GeV by ± 0.1 GeV and the renormalization scale $\mu = 4.8$ GeV by ± 1.2 GeV.

For light leptons($\ell = e, \mu$), we divide q^2 into five bins in maximum recoil region($0 \leq q^2 \leq 5$ GeV²) and calculate the semileptonic decay rates separately. The results are presented in Table II. We find that at small q^2 ($0 \leq q^2 \leq 1$ GeV²), the longitudinally polarized J/Ψ events dominate over the transversally polarized ones by a factor 8.5, and the difference will be reduced as q^2 increase. While for lepton τ , we divide q^2 into two bins($m_\tau^2 \leq q^2 \leq 4$, $4 \leq q^2 \leq 5$ GeV²) in maximum recoil region. Here the physical mass of lepton τ is taken to be $m_\tau^2 = 1.776^2$ GeV² [22], and the results are shown in Table III.

IV. CONCLUSIONS

The NLO semileptonic differential decay rates of B_c meson to charmonia are analyzed in detail with various choices of parameters. The uncertainties of partial decay widths in different bins of momentum transfer q^2 are discussed. For $B_c \rightarrow J/\Psi \ell \nu$ process, the partial decay widths for transverse and longitudinal polarizations are

investigated seperately. The distribution in the maximum recoil is found testable in the LHCb experiment, and in turn the NRQCD factorization will be also testified. To be noted that in the minimum recoil region, the NRQCD factorization is spoiled by the infrared divergences and hence is not applicable to analysis of those processes.

Acknowledgements:

This work was supported in part by the National Natural Science Foundation of China(NSFC) under the grants 10935012, 10821063 and 11175249.

Appendix A: The NLO B_c to Charmonia transition form factors

In this appendix, the QCD NLO B_c to charmonium transition form factors are given at the first order in power of m_c/m_b . For compactness of the expressions, we define $z = m_c/m_b$, $s = \frac{m_b^2}{m_b^2 - q^2}$, and $\gamma = \frac{m_b^2 - q^2}{4m_b m_c}$. Besides, the form factors at maximum recoil point, i.e. $q^2 = 0$, are also presented, which are in agreement with what given in references [19, 21].

$$\frac{f_+^{NLO}(q^2)}{f_+^{LO}(q^2)} = 1 + \frac{\alpha_s}{4\pi} \left\{ \frac{1}{3} (11C_A - 2n_f) \log\left(\frac{\mu^2}{2\gamma m_c^2}\right) - \frac{10n_f}{9} + \frac{(\pi^2 - 6 \log(2))(s-1) + 3s \log(\gamma)}{6s+3} \right\}$$

$$\begin{aligned}
& + \frac{C_A}{72s^2 - 18} \left(18s^2(2s-1)\log^2(s) + 18(8\log(2)s^3 - 2\log(2)s^2 - 5\log(2)s + s \right. \\
& + 2\log(2))\log(s) + (2s-1)(268s + \pi^2(6s^2 - 3s - 6) + 170) - 9(2s \\
& - 1)\log(\gamma)(\log(\gamma)s - (2 + 2\log(2))s + 4\log(2)) + 18(2s-1)(4s^2 + s \\
& - 2)\text{Li}_2(1-2s) - 18(4s^3 - 5s + 2)\text{Li}_2(1-s) + 18(s(4s(s+1) - 11) \\
& + 4)\log^2(2) - 36(5(s-1)s + 1)\log(2) \Big) \\
& + \frac{C_F}{6(1-2s)^2(2s+1)} \left(-6(2(s-1)s-1)\log^2(s)(1-2s)^2 + 3\log(\gamma)(23s \right. \\
& + (5s-2)\log(\gamma) - 4(s+1)\log(2) + 12)(1-2s)^2 - 12(4s^2 + s \\
& - 2)\text{Li}_2(1-2s)(1-2s)^2 + 12(s(2s+3) - 1)\text{Li}_2(1-s)(1-2s)^2 \\
& - (\pi - 2\pi s)^2(s(4s-19) + 4) + 3(-32\log^2(2)s^4 - 4(69 + 2\log(2))(-37 \\
& + 5\log(2)))s^3 + 8(18 + \log(2)(-31 + 9\log(2)))s^2 + (61 + 28\log(2) \\
& - 26\log^2(2))s + 12\log(2) + 2\log^2(2) - 32) + (6s(8s(s-4\log(2)s \\
& + 3\log(2) + 3) + 2\log(2) - 3) - 18\log(2) + 7) + 24\log(2))\log(s) \Big) \}, \tag{A1}
\end{aligned}$$

$$\begin{aligned}
\frac{f_+^{NLO}(0)}{f_+^{LO}(0)} &= 1 + \frac{\alpha_s}{4\pi} \left\{ \frac{1}{3}(11C_A - 2n_f)\log\left(\frac{2\mu^2}{m_b m_c}\right) - \frac{10n_f}{9} - \frac{1}{3}\log(z) - \frac{2\log(2)}{3} \right. \\
& + C_F \left(\frac{1}{2}\log^2(z) + \frac{10}{3}\log(2)\log(z) - \frac{35}{6}\log(z) + \frac{2\log^2(2)}{3} \right. \\
& + 3\log(2) + \frac{7\pi^2}{9} - \frac{103}{6} \Big) \\
& + C_A \left(-\frac{1}{6}\log^2(z) - \frac{1}{3}\log(2)\log(z) - \frac{1}{3}\log(z) + \frac{\log^2(2)}{3} \right. \\
& \left. \left. - \frac{4\log(2)}{3} - \frac{5\pi^2}{36} + \frac{73}{9} \right) \right\}, \tag{A2}
\end{aligned}$$

$$\begin{aligned}
\frac{f_0^{NLO}(q^2)}{f_0^{LO}(q^2)} &= 1 + \frac{\alpha_s}{4\pi} \left\{ \frac{1}{3}(11C_A - 2n_f)\log\left(\frac{\mu^2}{2\gamma m_c^2}\right) - \frac{10n_f}{9} + \frac{\log(\gamma)}{3} \right. \\
& + \frac{C_A}{36s-18} \left(-6\text{Li}_2(1-s)(1-2s)^2 + 6\log^2(2)(1-2s)^2 + 6s(2s-1)\log^2(s) \right. \\
& + (2s-1)(\pi^2(2s-3) + 146) + (12s\log(2)(4s-3) + 6\log(2) - 6)\log(s) \\
& - 3(2s-1)\log(\gamma)(\log(4\gamma) - 2) + 6(8s^2 - 6s + 1)\text{Li}_2(1-2s) - 12s\log(2) \Big) \\
& + \frac{C_F}{18(1-2s)^2(s-1)} \left(-6(s-1)(2s-3)\log^2(s)(1-2s)^2 \right. \\
& - 12(s-1)(4s-1)\text{Li}_2(1-2s)(1-2s)^2 + 24(s^2-1)\text{Li}_2(1-s)(1-2s)^2 \\
& - 6(-6s(2s(3s-8) + 11) + 2s(4s(s(4s-9) + 7) - 9)\log(2) + 2\log(2) + 13)\log(s) \\
& + (s-1)(3\log(\gamma)(3\log(\gamma) - 8\log(2) + 35)(1-2s)^2 - 24(s+2)\log^2(2)(1-2s)^2 \\
& \left. \left. - (2s-1)(546s + \pi^2(8s^2 - 34s + 15) - 279) + 24(s(43s-42) + 10)\log(2)) \right) \right\}, \tag{A3}
\end{aligned}$$

$$\frac{f_0^{NLO}(0)}{f_0^{LO}(0)} = \frac{f_+^{NLO}(0)}{f_+^{LO}(0)}, \tag{A4}$$

$$\begin{aligned}
\frac{V^{NLO}(q^2)}{V^{LO}(q^2)} &= 1 + \frac{\alpha_s}{4\pi} \left\{ \frac{1}{3}(11C_A - 2n_f)\log\left(\frac{\mu^2}{2\gamma m_c^2}\right) - \frac{10n_f}{9} \right. \\
& \left. - \frac{C_A}{36s-18} \left(9s(2s-1)\log^2(s) + 18(2s\log(2)(2s-1) + 1)\log(s) \right. \right.
\end{aligned}$$

$$\begin{aligned}
& +3\pi^2(s+2)(2s-1) - 2s(-18\log^2(2)s + 9\log^2(2) + 45\log(2) + 134) \\
& +9(2s-1)(\log(\gamma) - 3)\log(\gamma) + 18s(2s-1)(2\text{Li}_2(1-2s) - \text{Li}_2(1-s)) \\
& +63\log(2) + 134) \\
& + \frac{C_F}{6(1-2s)^2(s-1)} \left(6(s^2-1)\log^2(s)(1-2s)^2 + 24(s-1)s\text{Li}_2(1-2s)(1-2s)^2 \right. \\
& + 3(2s(s(4s(4\log(2)s - 8\log(2) + 3) + 20\log(2) - 17) - 4\log(2) + 7) - 1)\log(s) \\
& + (s-1)(6\log(\gamma)(\log(\gamma) - 6\log(2) + 5)(1-2s)^2 + 6(2s-9)\log^2(2)(1-2s)^2 \\
& + (2s-1)(-204s + 2\pi^2(2s^2 + s - 1) + 105) + 6(s(68s - 67) + 16)\log(2)) \\
& \left. - 12(2s^2 - 3s + 1)^2\text{Li}_2(1-s) \right) \}, \tag{A5}
\end{aligned}$$

$$\begin{aligned}
\frac{V^{NLO}(0)}{V^{LO}(0)} &= 1 + \frac{\alpha_s}{4\pi} \left\{ \frac{1}{3}(11C_A - 2n_f)\log\left(\frac{2\mu^2}{m_b m_c}\right) - \frac{10n_f}{9} \right. \\
& + C_F \left(\log^2(z) + 10\log(2)\log(z) - 5\log(z) + 9\log^2(2) \right. \\
& + 7\log(2) + \frac{\pi^2}{3} - 15) \\
& + C_A \left(-\frac{1}{2}\log^2(z) - 2\log(2)\log(z) - \frac{3}{2}\log(z) - 3\log^2(2) \right. \\
& \left. \left. - \frac{3\log(2)}{2} - \frac{\pi^2}{3} + \frac{67}{9} \right) \right\}, \tag{A6}
\end{aligned}$$

$$\frac{A_1^{NLO}(q^2)}{A_1^{LO}(q^2)} = \frac{A_2^{NLO}(q^2)}{A_2^{LO}(q^2)} = \frac{V^{NLO}(q^2)}{V^{LO}(q^2)}, \tag{A7}$$

$$\begin{aligned}
\frac{A_0^{NLO}(q^2)}{A_0^{LO}(q^2)} &= 1 + \frac{\alpha_s}{4\pi} \left\{ \frac{1}{3}(11C_A - 2n_f)\log\left(\frac{\mu^2}{2\gamma m_c^2}\right) - \frac{10n_f}{9} \right. \\
& + \frac{C_A}{72(s-1)s(2s-1)} \left(-9(s-1)s(2s-1)(2s+1)\log^2(s) - 9(2s(2s(\log(2)(4s^2-9) \right. \\
& + 3) + 12\log(2) - 3) - 4\log(2) - 2)\log(s) + (s-1)(-18(2s-1)\log^2(2)(s(2s+9) - 4) \\
& - (2s-1)(s(3\pi^2(2s+9) - 608) + 36) - 9(2s-1)\log(\gamma)(2\log(\gamma)s + 8\log(2)s - 6s \\
& + \log(\gamma) - 4\log(2) - 3) + 9(4s(13s-7) - 3)\log(2)) - 36(s(4s^3 - 9s + 6) - 1)\text{Li}_2(1-2s) \\
& + 18(s-1)(2s-1)(s(2s+5) - 2)\text{Li}_2(1-s) \Big) \\
& + \frac{C_F}{24s(2s^2 - 3s + 1)^2} \left(2\pi^2(1-2s)^2(s(2s-1) + 3)(s-1)^2 \right. \\
& + 24(1-2s)^2(s(2s+3) - 1)\text{Li}_2(1-2s)(s-1)^2 + 6s(2s+5)(2s^2 - 3s + 1)^2\log^2(s) \\
& + 3(s(2s(2s\log(2)(2s(76s-193) + 289) + 4s(-120s^2 + 369s + (8s^3 - 52s^2 + 90s - 43)\log^2(2) \\
& - 406) - 84\log^2(2) - 28\log(2) + 747) + 92\log^2(2) - 110\log(2) - 116) + 16\log^2(2) \\
& + 4(7 - 9\log(2))\log(2) - 3) + 3(s(2s(s(2s(4s(4\log(2)s - 6\log(2) + 6) - 28\log(2) - 69) \\
& + 156\log(2) + 113) - 2(13 + 58\log(2))) + 72\log(2) - 5) - 8\log(2) + 1)\log(s) \\
& - 6(2s^2 - 3s + 1)^2(16\log(2)s - 22s - 2\log(\gamma) + 4\log(2) + 1)\log(\gamma) \\
& \left. \left. - 12(2s^2 - 3s + 1)^2(2s^2 + s - 2)\text{Li}_2(1-s) \right) \right\}, \tag{A8}
\end{aligned}$$

$$\begin{aligned}
\frac{A_0^{NLO}(0)}{A_0^{LO}(0)} &= 1 + \frac{\alpha_s}{4\pi} \left\{ \frac{1}{3}(11C_A - 2n_f)\log\left(\frac{2\mu^2}{m_b m_c}\right) - \frac{10n_f}{9} + C_F \left(\frac{1}{2}\log^2(z) - \frac{119}{8} \right. \right. \\
& \left. \left. + 7\log(2)\log(z) - \frac{21}{4}\log(z) + 7\log^2(2) + \frac{15\log(2)}{4} \right) \right\}
\end{aligned}$$

$$+C_A\left(-\frac{3}{8}\log^2(z)-\log(2)\log(z)-\frac{9}{8}\log(z)-\frac{7\pi^2}{24}+\frac{67}{9}-\frac{9\log^2(2)}{4}+\frac{3\log(2)}{8}\right)\}. \quad (\text{A9})$$

-
- [1] F. Abe, et al. (CDF Collaboration), Phys. Rev. Lett. **81**, 2432 (1998); F. Abe, *et al.*, Phys. Rev. D**58**, 112004 (1998).
 - [2] D. Lucchesi, in ICHEP 2004, ed. H. Chen, *et al.*, World Scientific, Singapore, 2005, p158.
 - [3] N. Brambilla, *et al.*, (Quarkonium Working Group), CERN-2005-005, [arXiv:hep-ph/0412158].
 - [4] C.-H. Chang, C. Driouichi, P. Eerola and X.-G. Wu, Comput. Phys. Commun. **159**, 192 (2004).
 - [5] P. del Amo Sanchez, et al. (BABAR Collaboration), Phys. Rev. D**83**, 032007 (2011).
 - [6] Patricia Ball and Roman Zwicky, Phys. Rev. D**71**, 014015 (2005).
 - [7] Patricia Ball and Roman Zwicky, Phys. Rev. D**71**, 014029 (2005).
 - [8] V. V. Kiselev, A. E. Kovalsky, and A. K. Likhoded, Nucl. Phys. B**585**, 353 (2000).
 - [9] I. P. Gouz, V. V. Kiselev, A. K. Likhoded, V. I. Romanovsky, and O. P. Yushchenko, Phys. Atom. Nucl.**67**, 1559 (2004); Yad. Fiz. 67, 1581 (2004).
 - [10] T. Huang and F. Zuo, Eur. Phys. J. C**51**, 833 (2007).
 - [11] T. Huang, Z.-H. Li, X.-G. Wu, and F. Zuo, Int. J. Mod. Phys. A**23**, 3237 (2008).
 - [12] M. A. Ivanov, J. G Körner, and P. Santorelli, Phys. Rev. D**63**, 074010 (2001); Phys. Rev. D**73**, 054024 (2006).
 - [13] D. Ebert, R. N. Faustov, and V. O. Galkin, Phys. Rev. D**68**, 094020 (2003).
 - [14] C.H. Chang and Y.Q. Chen, Phys. Rev. D **49**, 3399 (1994).
 - [15] W. Wang, Y.L. Shen, and C.D. Lü, Phys. Rev. D **79**, 054012 (2009).
 - [16] E. Hernandez, J. Nieves, and J. M. Verde-Velasco, Phys. Rev. D**74**, 074008 (2006).
 - [17] K. K. Pathak and D. K. Choudhury, [arXiv:hep-ph/1109.4468].
 - [18] M. Wirbel, B. Stech, and M. Bauer, Z. Phys. C**29**, 637 (1985); M. Bauer, B. Stech, and M. Wirbel, Z. Phys. C**34**, 103 (1987).
 - [19] Guido Bell, Ph.D. Thesis, [arXiv:hep-ph/0705.3133].
 - [20] G. Bell and Th. Feldmann, Nucl. Phys. Proc. Suppl.**164**, 189-192 (2007).
 - [21] C.-F. Qiao, P. Sun and F. Yuan, JHEP **1208**, 087 (2012).
 - [22] K. Nakamura, *et al.*, (Particle Data Group), J. Phys. G **37**, 075021(2010).
 - [23] E. J. Eichten and C. Quigg, Phys. Rev. D**49**, 5845-5856(1994).
 - [24] C.-F. Qiao, L.-P. Sun, and R.-L. Zhu, JHEP **1108**, 131 (2011).